Thermal Stability and Electrical Properties of boron- and phosphorus-doped hydrogenated silicon and germanium multilayers in nanoscale

Ibrahim A. Saleh[1], Tarek M. Fayez[*2], Mustafah M. A. Ahmad[2]
[1]Physics Department, Faculty of Science, Benghazi University, Libya
[2]School of physics, Sebha University, Libya
*Corresponding author: tar.ahmad@sebhau.edu.ly

***Abstract*-We report the synthesis, structure and electrical properties in boron- and phosphorus-doped hydrogenated silicon and germanium multilayers (P- a-Si:H/a-Ge:H and B-doped a-Si:H/a-Ge:H) , with the activation energy of crystallization of the P-and B-doped are 42.15 and 67.6 kJ/mol, respectively. In this materials, the incorporation of boron or phosphorus leads to decrease activation energies of crystallization and an increase of the conductivity. The photo-electrical conductivity increases more rapidly than dark - electrical conductivity which confirms the sensitive thin film for light.**

Keywords: Doped, nano-multilayers (NMLs), a-Si:H/a-Ge:H, hydrogen dilution, structure, electrical conductivity, crystallization, Avrami's equation

I. INTRODUCTION

A tremendous advance in applications of amorphous semiconducting thin films has been achieved in the field of optoelectronic devices. Hydrogen is the element of choice to passivate dangling bonds in amorphous semiconductors, like Si and Ge because of its single-electron atomic structure. By hydrogenation better optoelectronic properties are obtained. In this regard, hydrogenated amorphous silicon (a-Si:H) and hydrogenated amorphous germanium (a-Ge:H) thin films are key materials for employment in (nano) structures used, e.g., in the technology of multi-junction solar cells where a-Ge:H acts as the low-band gap absorber while a-Si:H acts as the high-band gap one, thus allowing a better exploitation of the solar spectrum and the achievement of higher efficiencies [1-3].
The a-SiGe:H alloy is now the material of choice as the low-band gap absorber used in solar cells. It allows a higher degree of freedom to control the optical band gap over some range by changing the Si/Ge ratio [4,5]. The a-SiGe:H alloys can be deposited from a sequence of ultrathin a-Si:H and a-Ge:H layers by intermixing them [1,6,7], which is obtained by heat treatments. The heat treatments are often also used for activating dopants. The doped multilayers, e.g., p-layer doped with boron (p-a-Si:H/Ge:H multilayers) and n-layer doped with phosphorus (n-a-Si:H/Ge:H multilayers) can be prepared by four chamber glow-discharge deposition system and then annealed to produce intermixing also. The main objective of doping a-Si:H/a-Ge:H multilayers is to modify its electrical conductivity in order to establish an electrical field necessary for a correct extraction of the electrons generated in the intrinsic film. Concerning the p-layer, the optimum conductivity is generally achieved by mixing the source gas (SiH4, GeH4) with diborane (B2H6) [8], and the n-layer, achieved by mixing the source gas (SiH4,GeH4) with phosphorus (PH3). However boron or phosphorus tends to alloy with a-Si:H/a-Ge:H multilayers leading to a strong reduction in the band gap. However, the behavior of H is not fully understood and predictable when the materials are submitted to illumination or thermal treatment [9]. Previous studies have shown that the hydrogen content and annealing conditions can dramatically influence the structural stability of the a-SiGe:H and a-Si:H/a-Ge:H multilayers.It was reported that surface bumps formed, size and height, increased with increasing H content and/or annealing temperature and time [9]. The craters also formed subsequent to the explosion of the bumps. The bumps were ascribed to the formation of bubbles of hydrogen in of the a-Si/a-Ge multilayers [10-12]. The formation of H bubbles was also suggested by Acco et al. [13] in single layers of a-Si. It was hypothesized that H could be first released from the Ge layers because of the lower binding energy of the Ge-H bond with respect to the Si-H one [11,13].
The most convenient method to deposit these materials is by four chamber glow-discharge deposition system. In this method the substrate temperatures should not exceed a certain level (typically between 200 and 250°C) to prevent hydrogen desorption, which will affect the otherwise excellent passivation of grain boundary defects. This method has gained popularity because the deposition may be carried out at various temperatures and is thus suitable for use of wide spectrum of substrate materials like, quartz, silicon wafers etc. The properties of the materials deposited by this method depend very sensitively on the deposition parameters [14].

II. EXPERIMENTAL

The boron (B) and phosphorous (P) doped a-Si:H/a-Ge:H multilayers was deposited by alternating deposition from SiH4 and GeH4 plasmas mixed with B2H4 or PH3 gases, respectively in a computer-controlled four chamber glow-

discharge deposition system with capacitive coupled diode reactors. At a substrate temperature of 200°C, a RF of 13.6 MHz, a RF power of 10 W, a pressure of about 0.18 mbar and a gas flow of 5 sccm in the SiH4 chamber and 0.32 mbar and a gas flow of 0.25-2 sccm of GeH4 mixed with 1% B2H4 to prepare p-type and a gas flow of 0.25-2 sccm of GeH4 doped with 1% PH3 for preparing n-type a-Si:H/a-Ge:H multilayers, P- and B-doped multilayers, with barrier layer thickness of 3 nm and well layer thickness of 2.8 and 3 nm were prepared for the measurements. The individual thickness of a-Si:H barrier layer dSi was varied by changing the deposition time, while the well layer thickness dGe of a-Ge:H was controlled by changing the hydrogen dilution ratio [H2]/[GeH4] as well as by changing the deposition time. The growth rate was kept near 0.1 nms-1for a-Si:H and ranged from 0.1 to 0.4 nms-1 for a-Ge:H layers.The total film thickness measured by the dektak surface profiler was in the range of 300 to 550 nm and the total number of periods was controlled between 60 and 100.

III. Results and Discussion

A. *Infrared absorption spectra*

Infrared absorption spectra were measured in the range between 400 and 2200 cm-1 using a Nicolet Fourier transform infrared spectrometer (model 740). After base line correction, the IR absorption peaks were fitted by Gaussian to obtain the integrated absorption intensity I*. As the film thickness was usually below 1 μm, the correction proposed by Langford et al. was employed to obtain the integrated absorption I. The optical band gap Eg was deduced from transmission and reflection measurements using JASCO V-570 UV - vis Spectrophotometer–Instructions.

Typical infrared (IR) absorption spectra for a-Si:H(3 nm)/a-Ge:H multilayers of dGe=2.8 nm doped with P and of dGe= 3 nm doped with B are shown in Figure 1. the absorption peak near1880 cm-1 is attributed to the stretching vibration of Ge-H groups incorporated into bulk material, while the absorption near 2100 cm-1 is associated with the vibration of Si-H and/or Si-H2 groups located at internal surfaces of voids. The absorption peak near 2000 cm-1 was attributed to Ge-H or Ge-H2 groups at void surface and Si-H groups in compact material [15,16-18]. It is seen that after annealing for 8 h at 300oC, the absorbance integrated intensity of the waging, bending and stretching bond decreases for the two samples. In the stretching mode range of the wave number, the spectra show that the integrated absorption intensity of Ge-H and Si-H stretching bonds is decreasing after annealing at 300oC, indicating that hydrogen moves around in Ge layers and is partially evolved, thus causing a change in the atomic density of the Ge network and also a change in the ratio of dGe/(dSi+ dGe) which is correlated with the structure factor [19]. The hydrogen evolved from Ge leads to structural relaxation caused by the annealing preferentially occurs [17,20,21,22-24].

The hydrogen content (NH) of P- and B-doped a-Si:H(3 nm)/a-Ge:H multilayers of dGe =2.8 and 3 nm calculated by fitting the stretching mode Figures (2) and (3) , before and after annealing at 300°C for 8 h is given in Table I. The fitting was done by using the Gaussian distribution. For brevity see Figure 4, for B- doped a-Si:H/a-Ge:H multilayers before annealing. It is seen from Table I, that the total hydrogen content (NH) is decreased after annealing due to the evolution of hydrogen from the network and producing bubbles on the surface of the films as are shown by SEM.

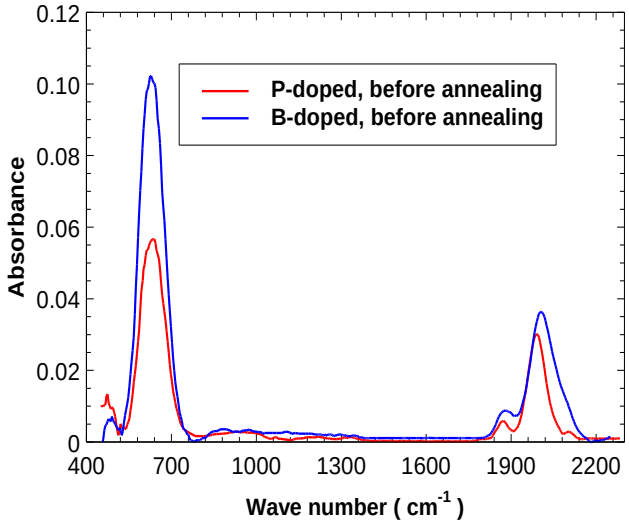

Fig.1. IR- spectra of untreated P- and B- doped a-Si:H(3 nm)/a-Ge:H multilayers of d_{Ge}= 2.8 and 3 nm.

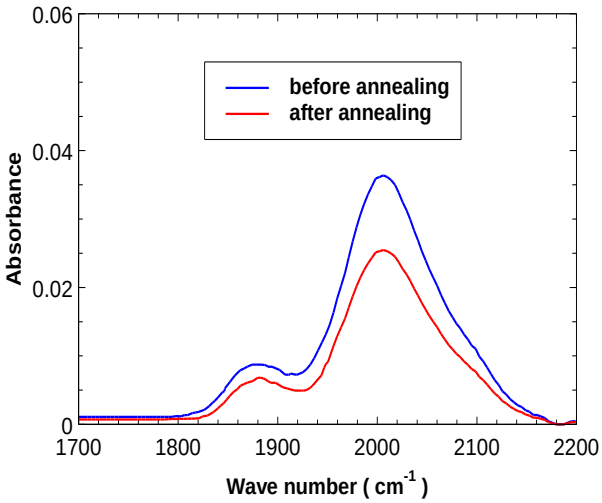

Fig.2. IR- spectra in the stretching mode of P- doped a-Si:H(3 nm)/a-Ge:H multilayers of d_{Ge}=2.8 nm before and after annealing at 300°C for 8 h.

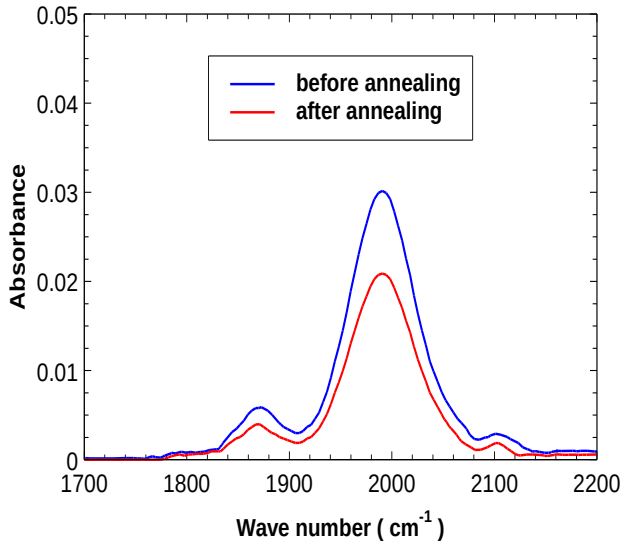

Fig. 3. IR-spectra in the stretching mode for B-doped a-Si:H(3nm)/a-Ge:H multilayers of d_{Ge}= 3 nm before and after annealing at 300°C for 8 h.

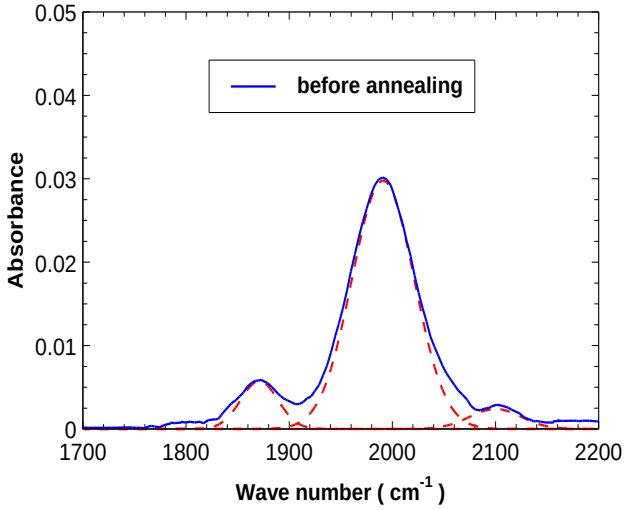

Fig. 4. Fitting of IR- spectra in the stretching mode range for B-doped a-Si:H(3 nm)/a-Ge:H multilayers of d_{Ge}= 3 nm before annealing at 300°C for 8 h.

TABLE I: THE HYDROGEN CONTENT FOR THE TWO SAMPLES BEFORE AND AFTER ANNEALING.

The samples	**Hydrogen content (N_H) cm^{-3} before annealing**	**Hydrogen content (N_H) cm^{-3} after annealing**
P-doped a-Si:H(3 nm)/a-Ge:H	2.97 x10^{21}	2.03 x10^{21}
B-doped a-Si:H(3 nm)/a-Ge:H	3.98 x10^{21}	2.70 x10^{21}

B. The X-ray diffraction (XRD)

The structural change of P-doped a-Si:H(3 nm)/a-Ge:H multilayers (n-type) of dGe=2.8 nm after annealing at 300°C for 8 h have been investigated by XRD. The phases appeared in the x-ray spectra are Ge-Ge(211), Ge-Ge(220), Ge-Ge(400) and Ge-Ge(332). The crystallization occurs in a-Ge:H layers only because the crystallizing temperature of germanium at 300°C is lower than that of silicon near 550°C. Similarly the structural changes for B-doped a-Si:H(3 nm)/a-Ge:H multilayers (p-type) of dGe= 3 nm annealed at 300°C for 8 h have been investigated by XRD. The phases appeared in the x-ray spectra are Ge- Ge(411) phases only. As reported the crystallization occurs in the a-Ge:H layers only because the crystallizing temperature of the germanium at 300°C is lower than that of silicon.

C. Scanning electron microscopy (SEM)

The P- and B-doped a-Si:H (3nm)/a-Ge:H multilayers annealed at 300°C for 8 h were characterized by the scanning electron microscopy (SEM) as shown in Figures (5) and (6), respectively. It is seen from the images that bumps appear on the surface of the films annealed at 300°C for 8 h. The rupture of the Si-H and Ge-H bonds doped by thermal energy to the annealing temperature is the main reason for the formation of hydrogen which in turn is the bubbles [23,25].

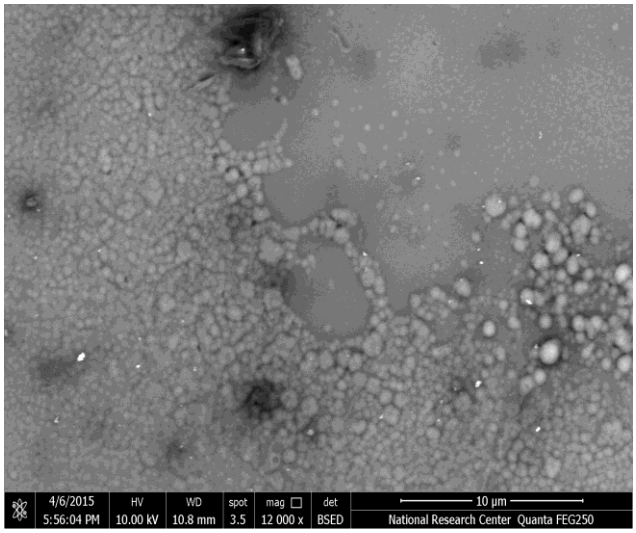

Fig. 5. SEM images for P-doped a-Si:H(3 nm)/a-Ge:H multilayers of d_{Ge}=2.8 nm after annealing at 300°C for 8 h.

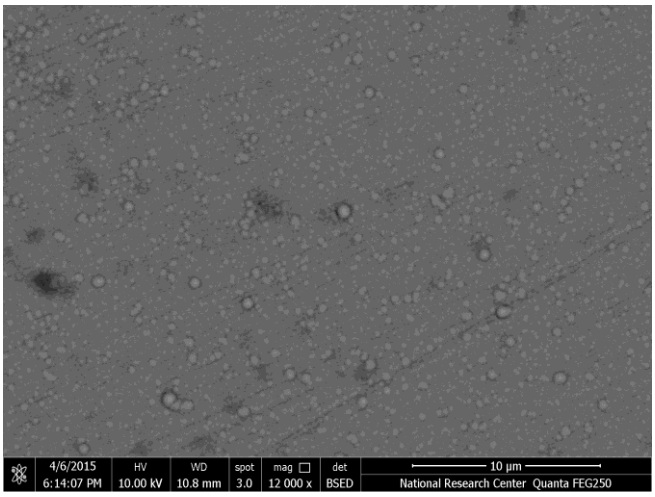

Fig. 6. SEM images for B-doped a-Si:H(3 nm)/a-Ge:H multilayers of d_{Ge}= 3 nm after annealing at 300°C for 8 h.

D. Electrical properties

1. Temperature dependence of the electrical conductivity

The dark and photo-electrical conductivity as a function of temperature for P- and B- a-Si:H(3nm)/a-Ge:H multilayers in the temperature range 303-443 K is shown in Figures (7) and (8), respectively. It is seen that the relation between the electrical conductivity and the temperature obey the Arrhenius type equation [18]:

$$\sigma = \sigma_0 \, exp\,(-E_a/k_B T) \qquad (1)$$

where σ is electrical conductivity, Ea is the activation energy and kB is the Boltzmann`s constant.

The conductivity measured at 303 K and the activation energy calculated from the slopes of the lines is given in Table II. It seen that the phosphors incorporation induced an improvement of the dark electrical conductivity (σd) with a decrease of its activation energy. These results can be related to the shift of the Fermi level towards the conduction band due to phosphors doping. Also the boron incorporation induced an increase of the electrical conductivity and a less decrease of its activation energy which is due to the shift of Fermi level towards the valence band upon boron doping. The electrical measurements under white light showed that the incorporated phosphors or boron conducts to a degradation of the light sensitivity of the films [18,26].

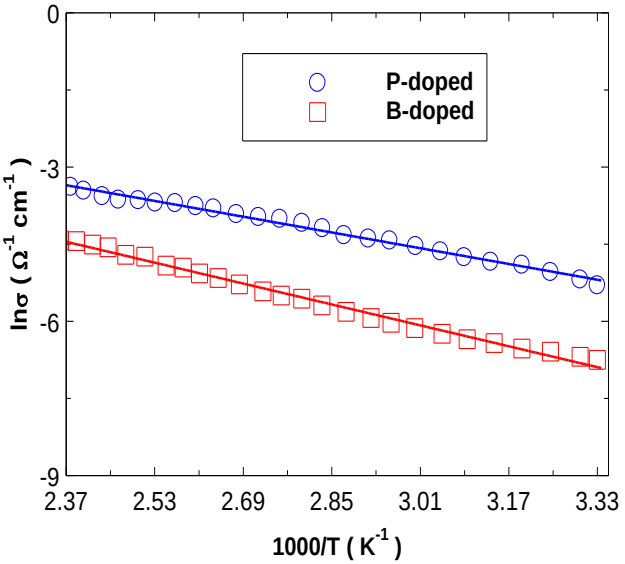

Fig. 7. Logarithm of dark- electrical conductivity vs. inverse of temperature for P- and B- a-Si:H(3 nm)/a-Ge:H multilayers.

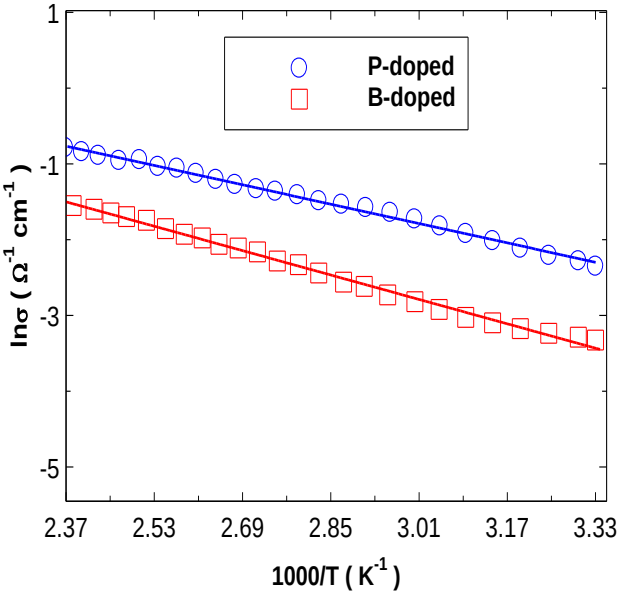

Fig. 8. Logarithm of photo- electrical conductivity Vs. inverse of temperature for P- and B- a-Si:H(3 nm)/a-Ge:H multilayers.

TABLE II . THE DARK AND PHOTO-ELECTRICAL CONDUCTIVITY AT 303 K AND THE ACTIVATION ENERGY FOR A-SI:H(3 NM)/A-GE:H MULTILAYERS OF THICKNESS DGE=2.8 NM (P-DOPED) AND DGE= 3 NM (B-DOPED).

Samples	$\sigma_d(\Omega^{-1}.cm^{-1})$	$\sigma_{Ph}(\Omega^{-1}.cm^{-1})$	σ_{Ph}/σ_d	$E_{a,d}$ (e.V)	$E_{a,Ph}$ (e.V)
(P-doped)	5.19 X 10^{-3}	8.89 X 10^{-1}	17	0.16	0.14
(B-doped)	1.11 X 10^{-3}	3.44 X 10^{-1}	31	0.22	0.17

2. *Kinetics and influence of annealing time on electrical conductivity*

The dark conductivity as a function of the annealing time at constant temperatures (less than the substrate temperature Ts) for P- and B- doped a-Si:H(3 nm)/a-Ge:H multilayers are shown in the figures (9) and (10), respectively. The increase of dark electrical conductivity with increasing the annealing time at constant temperatures 323 K, 373 K and 423 K is due to release of weak-bonded hydrogen from internal surface voids [19,27,28]. The change of dark and photo-electrical conductivity with the annealing time at temperatures 323 K is shown in Figures (11) and (12), respectively. It is seen that the photo-electrical conductivity increases more rapidly than dark - electrical conductivity which conforms the sensitive thin film for light.

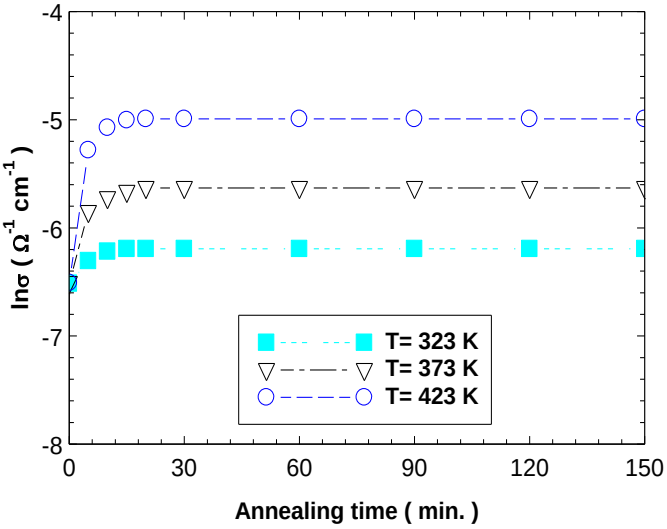

Fig. 9.logarithm of the electrical conductivity versus the annealing time at constant temperatures for P-doped a-Si:H(3nm)/a-Ge:H multilayers of d_{Ge}=2.8 nm.

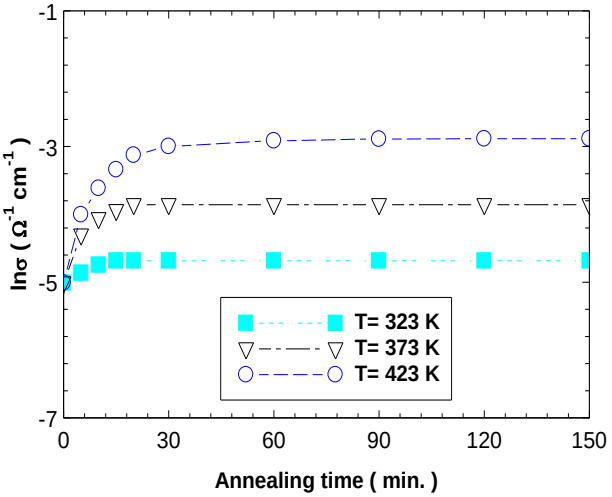

Fig. 10. Logarithm of the electrical conductivity versus the annealing time at constant temperatures for B-doped a-Si:H(3 nm)/a-Ge:H multilayers of d_{Ge}= 3 nm.

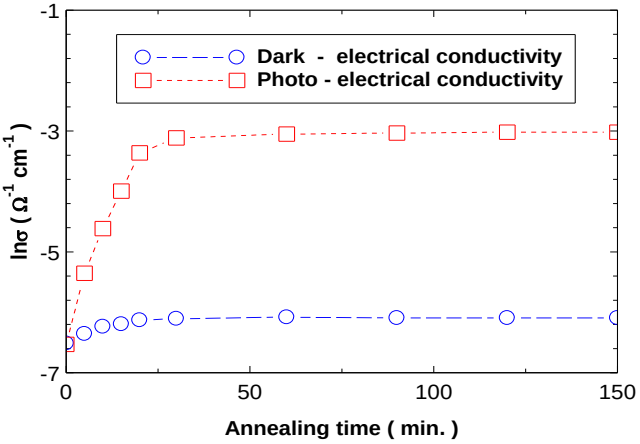

Fig. 11.logarithm of the dark and photo-electrical conductivity versus annealing time at constant temperature 323K for P-doped a-Si:H(3nm)/a-Ge:H multilayers of d_{Ge}=2.8 nm.

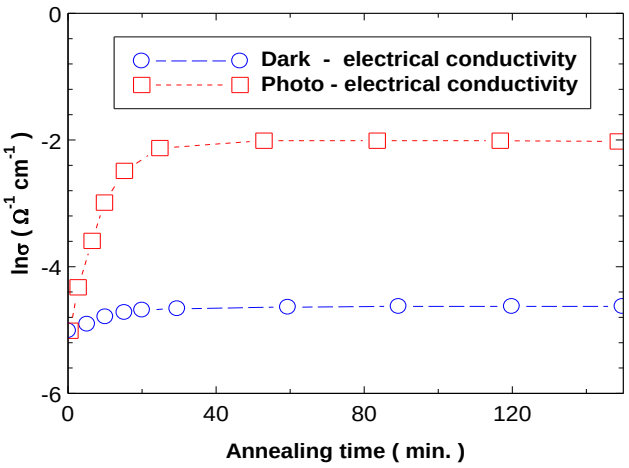

Fig. 12. logarithm of the dark and photo- electrical conductivity vesus annealing time at constant temperature 323 K for B-doped a-Si:H(3nm)/a-Ge:H multilayers of d_{Ge}=3 nm.

The electrical conductivity and the activation energy for P and B-doped a-Si:H/a-Ge:H multilayers is affected by annealing temperature while the electrical conductivity increases and the activation energy decreases noticeably due to dopant segregation. This means that the phosphors or boron atoms passivated by hydrogen can be activated from the annealing temperature through bridging Ge-H----P and Ge-H---B bonds dissociation [19,26].

The same behavior was obtained for films annealed at constant temperature higher than the substrate temperature as shown in Figures (13) and (14). In this case the increase of dark conductivity can be attributed partially to crystallization in Ge layers and partially to a release of hydrogen from the films. The crystallization occurs in the germanium layers only because of the weak bonds between germanium and hydrogen atoms and a low crystallization temperature of Ge (near 300ºC) as confirmed by X-ray data (section.3.2.).

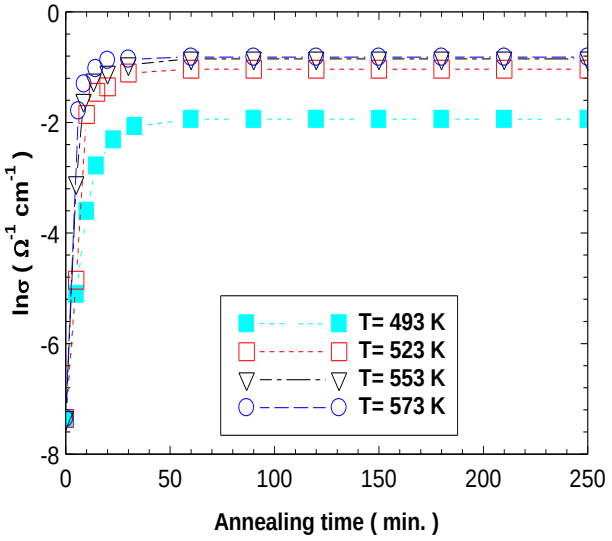

Fig. 13. Logarithm of dark electrical conductivity versus the annealing time at constant temperatures for P-doped a-Si:H(3 nm)/a-Ge:H multilayers of d_{Ge}=2.8 nm.

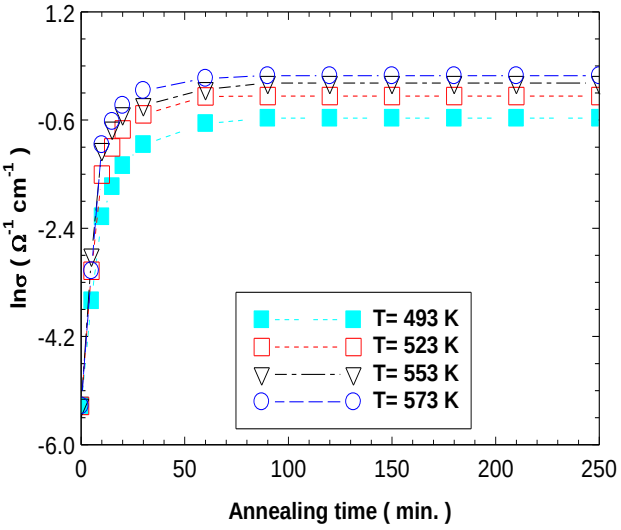

Fig. 14.logarithm of dark electrical conductivity versus annealing time at constant annealing temperatures for B-doped a-Si:H(3 nm)/a-Ge:H multilayers of d_{Ge}= 3 nm.

Thus the electrical conductivity measurements as a function of annealing time at constant temperature are used to study the isothermal crystallization kinetics using Johnson-Mehl-Avermi`s (JMA) equation [29] in the form:

$$\chi = 1 - exp[-kt^n] \quad (2)$$

Where χ is the volume fraction of the crystalline phases transformed from the amorphous state at time t, n refers to the order of reaction and k is the effective overall reaction rate, which actually reflects the rate of crystallization [30, 31] and is given by:

$$k = k_o \, exp\,[-E_c/RT] \quad (3)$$

Here k_o indicates the number of attempts to overcome the energy barrier. The electrical conductivity as a function of annealing time the volume fraction χ is:

$$\chi = (Ln\ \sigma_a - Ln\sigma_t)/(Ln\sigma_a - Ln\sigma_c) \quad (4)$$

where $Ln\sigma_a$ is logarithm of the electrical conductivity at zero time (activation electrical conductivity), Ln σ_t logarithm of the electrical conductivity at any time t and ln σ_c is logarithm of the electrical conductivity at the end of saturation (full crystallization). According to JMA equation the value of n can be obtained from the slopes of the plots of Ln[-Ln(1-χ)] vs. Ln t are measured at dark and light for this material. Since the volume fraction of the crystallized phases is assumed to depend on the electrical conductivity of the material at any annealing time, the value of n can depend on the composition and annealing temperature in this study. The values of k according to JMA equation are obtained from the slopes of the plots of $-\ ln(1-\ \chi)\ vs.\ (t^n)$. According to equation (3) the values of the activation energies E_c of crystallization can be deduced from the slopes of the plots of Lnk versus 1000/T.

According to JMA equation the results obtained for n, k and the activation energy E_c of crystallization for P- and B-doped a-Si:H(3 nm)/a-Ge:H multilayers measured at 493, 523, 553 and 573 K are given in Table III. It is seen that the activation energy of crystallization for B-doped films is higher than that of P-doped as confirmed by X-ray data.

TABLE III. VALUES OF N, K AND EC FOR A-SI:H(3 NM)/A-GE:H MULTILAYERS OF THICKNESS DGE=2.8 NM (P-DOPED) AND DGE= 3 NM (B-DOPED).

	n				K				
T / **Type**	493 (K)	523 (K)	553 (K)	573 (K)	493 (K)	523 (K)	553 (K)	573 (K)	E_c kJ/mol
P-doped	0.738	0.689	0.668	0.611	$1.31x10^{-2}$	$2.65x10^{-2}$	$3.59\ x10^{-2}$	$6.01x10^{-2}$	42.15
B-doped	0.860	0.796	0.683	0.544	$5.31x10^{-3}$	$7.53x10^{-3}$	$1.52\ x10^{-2}$	$6.45x10^{-2}$	67.60

IV. Conclusion

The change of dark and photo-electrical conductivity with the annealing time at temperatures 323 K reveal that, the photo-electrical conductivity increases more rapidly than dark - electrical conductivity which confirms the sensitive thin film for light. The elements of dopes, plays an important role in affecting for the activation energies of crystallization and electrical conductivity. The electrical conductivity and the activation energy is affected by annealing temperature, where the activation energy decrease and electrical conductivity increase with decrease the hydrogen content, and increasing of crystallizing with annealing time, that thing was appeared for P-doped more than for B-doped duo to P-doped is a donor material while B-doped is accepter material. The incorporation of boron or phosphorus leads to decrease activation energies of crystallization and an increase of the conductivity. The activation energy of crystallization of the P-and B-doped are 42.15 and 67.6 kJ/mol, respectively.

References

[1] E. P. Donovan, F. Spaepan, D. Turnbull, J. M. Poate, and D. C. Jacobson, J. of Appl. Phy., vol. 57, pp. 1795 (1985).

[2] G. G. Pethuraja, R. E. Welser, A. K. Sood, C. Lee, N.J. Alexander, H. Efstathiadis, P. Haldar, J. L. Harvey, Mater. Scie. Appi. vol. 3, pp. 67 (2012).

[3] X. Sun, T. Zhang, L. Yu, L. Xu, J. Wang, Scientific Reports 9, 19752 (2019).

[4] R. Sinclair, J. Morgiel, A. S. Kirtikar, I. W. Wu, and A. Chiang, Ultramicroscopy, vol. 51, pp. 41 (1993).

[5] G. L. Olson and J. A. Roth, Materials ScienceR eports,vol. 3, pp. 3-77 (1988).

[6] K. Zellama,P. Germain ,S. Squelard , J.C. Bourgoin, and P. A. Thomas, J. of Appl. Phys., vol. 50, pp. 6995- 7000 (1979).

[7] U. Koster, Physica Status Solidi A, vol. 48, pp. 313 (1978).

[8] M. K. Hatalis and D. W. Greve, J.of Appl. Phy. vol. 63, pp. 2260-2266 (1988).

[9] J. D. Cohen, Solar Energy Mater. Solar Cells, vol.78, pp. 399 (2003).

[10] C. Frigeri, L. Nasi, M. Serenyi, A. Csik, Z. Erdelyi, D.L. Beke, vol.45, pp. 475 (2009).

[11] A. Csik, M.Serenyi, Z. Erdelyi, A. Nemcsics, C. Cserhati, G.A. Langer, D.L. Beke, C. Frigeri, A. Simon, vol.84, pp.137 (2010).

[12] A.C. Frigeri,M. Serényi, A. Csik, Z. Erdélyi, D.L. Beke, L. Nasi, J Mater Sci Mater Electron, vol.19, pp. S289 (2008).

[13] S. Acco, D. L. Williamson, P.A. Stolk, F.W. Saris, M.J. van den Boogaard, W. C. Sinke, W. F. van der Weg, S. Roorda, P. C. Zalm, Phys. Rev. B, vol.53, pp. 4415 (1996).

[14] K. L. Chopra in "Thin Film phenomena" McGraw Hill Book company (1969).

[15] M. S. Abo Ghazala, Physica B 293, 132 (2000).

[16] K. W. Jobson and J.P.R. Wells,R.E. I. Schropp,N.Q. Vinh,J.I. Dijkhuis, J. Appl. Phys. 103, 13106 (2008).

[17] K. Chen, S. Huang, J. Xu, X. Huang, H. Fritzche, A. Matsuda, G. Gangul, Journal of optoelectronics and Advanced Materials, Vol.4,561(2002).

[18] M. S. Abo-Ghazala, P hys. Status Solidi C 8, 3099–3102 (2011).

[19] H. Xu, Y. Wang and G. Chen**,** phys. stat. sol. (a) 143, K87 (1994).

[20] M. Daouahi, K. Zellama, H. Bouchriha, P. Elkaïm, Eur Phys J AP10,185 (2000).

[21] Y. Bouizem , A. Belfedal, J.D. Sib , A. Kebab , L. Chahed , J Phys Condens Matter, 19,356215 (2007).

[22] S. Kannan, Master of Science**,** Department of Physics, the University of Utah (2005).

[23] C. Frigeri, M. Serenyi, Zs. Szekrenyes, K. Kamaras, A. Csik, N.Q. Khanh, Solar Energy 119, pp. 225-232 (2015).

[24] R.J. Soukup, N. J. Ianno, S. A. Darveau, C. L. Exstrom, Sol. Energy Mater.Sol. Cells 87,87 (2005).

[25] W. Beyer and V. Zastrow, J. Non-Cryst. Solids 227-230, 880 (1998).

[26] N. Khelifati, S. Tata1, A. Rahal, R. Cherfi, A. Fedala, M. Kechouane, and T. Mohammed-Brahim, Phys. Status Solidi C 7, 679–682 (2010).

[27] M. S. Abo Ghazala, E. Aboelhasn, A. H. Amar, and W. Gamel, Phys. Status Solidi C 8, No. 11–12, 3095–3098 (2011).

[28] A. A. D. T. Adikaaria and S. R. P. Silva, J. of Appl. Phys. Vol. 97, 114305 (2005).

[29] J. A. Augis, J. E. Bennett, J. Thermal Anal. 13, 283 (1978).

[30] M. M. EL-Zaidia, A. Shafi, A.A.Ammar, M. Abo-Ghazala, J. Mat. Sci. 22, 1618 (1987).

[31] Pradeep, N.S. SaxenaA. Kumar, Physica Scripta 54, 207 (1996).